Dynamic Efficient Adversarial Training Guided by Gradient Magnitude

Anonymous Author(s)
Affiliation
Address
email

Abstract

Adversarial training is an effective but time-consuming way to train robust deep neural networks that can withstand strong adversarial attacks. As a response to its inefficiency, we propose Dynamic Efficient Adversarial Training (DEAT), which gradually increases the adversarial iteration during training. We demonstrate that the gradient's magnitude correlates with the curvature of the trained model's loss landscape, which allows it to reflect the effect of adversarial training. Therefore, based on the magnitude of the gradient, we propose a general acceleration strategy, M+ acceleration, which enables an automatic and highly effective method of adjusting the training procedure. M+ acceleration is computationally efficient and easy to implement. It is suited for DEAT and compatible with the majority of existing adversarial training techniques. Extensive experiments have been done on CIFAR-10 and ImageNet datasets with various training environments. The results show that proposed M+ acceleration significantly improves the training efficiency of existing adversarial training methods while maintaining or even enhancing their robustness performance. This demonstrates that the strategy is highly adaptive and offers a valuable solution for automatic adversarial training.

1 Introduction

While deep neural networks (DNNs) continue to achieve better performance across a broad range of activities, their safety and dependability are getting increasing attention. These sophisticated models are known to be vulnerable to adversarial examples [6, 10, 15, 27], maliciously perturbed examples that can fool or mislead target DNNs but remain visually indistinguishable for humans, and adversarial training has been demonstrated as one of most effective defensive strategies to improve DNNs' adversarial robustness [2, 22]. The basic idea of adversarial training was proposed by Goodfellow et al. [11], which showed that the robustness of DNNs could be improved by injecting the adversarial examples into training data. Madry et al. [18] later formulated adversarial training as a Min-Max optimization problem (see Eq. (1)), which indicates that using high-quality adversarial examples as training data can boost the robust performance of trained models. However, it usually takes multiple backpropagation to generate such adversarial perturbations, which is computationally expensive. The prohibitive training cost has become one of the major challenges in adversarial training [32].

Aiming to improve the training efficiency, in this paper we take a closer look at existing adversarial training strategies [18, 24, 31] and find that redundant adversarial iterations could slow down the training process and sometimes even cause catastrophic forgetting [24], which

Submitted to 36th Conference on Neural Information Processing Systems (NeurIPS 2022). Do not distribute.

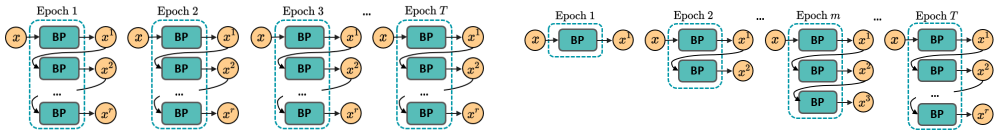

(a) FREE AT (b) DEAT

Figure 1: An Illustration of the acceleration brought by Dynamic Efficient Adversarial Training (DEAT). While FREE Adversarial Training (AT) performs a fixed number of adversarial iterations, DEAT enables a more efficient training paradigm by executing less backpropagation (BP), which is most computationally expensive operation in AT.

spoils the trained model's robustness. To reduce the redundant backpropagation, we design a flexible adversarial training strategy, called Dynamic Efficient Adversarial Training (DEAT), which begins the training with natural training data and gradually increases adversarial iterations when a pre-defined criterion is satisfied. Moreover, we show that the magnitude of a network's gradient with respect to training adversarial perturbations can roughly reflect the training effect and demonstrate that the model tends to gain 'robustness' after training if the gradient magnitude stays small. Based on such an observation, we design a self-adaptive criterion based on gradient magnitude for DEAT and further extend it as a general acceleration strategy that can directly boost the training efficiencies of other state-of-the-art adversarial training methods like [30, 36]. Experiments have been done on CIFAR-10 [16] and ImageNet [8] datasets with different model architectures, and the results demonstrate that our magnitude-guided strategy can significantly speed up adversarial training methods under different training environments and achieves comparable or even better robust performances than before acceleration.

2 Background and Related Works

General Notations Given a dataset D that contains N pairs of example and label (x_i, y_i), we denote by X a set of all $x \in D$, where the number of examples in X is written as $|X|$. Denoted by $F : \mathbb{R}^n \to \mathbb{R}^C$, a neural network classifier parameterized by θ takes $x \in \mathbb{R}^n$ as input and labels it into one of the C classes based on $\arg\max_{k=\{1,\dots,C\}} F_c(x;\theta)$. We denote by L the loss function that measures the difference between the model's predictions and ground truth labels and write $f(x;\theta)$ as a shorthand of $L(F(x;\theta), y)$ for simplicity. This paper focus on the ℓ_∞ threat model [18], *i.e.*, $\delta \in B_\epsilon$ is an adversarial perturbation added on x and B_ϵ is a ℓ_∞ norm ball with radio ϵ. A projection is represented by $\mathcal{P}_\epsilon$, which maps any input δ into B_ϵ.

Adversarial Training Adversarial Training (AT) produce robust classifier via optimizing a Min-Max problem,

$$\min_\theta \mathbb{E}_{(x,y)\in D}\big(\max_{\delta\in B_\epsilon} f(x+\delta;\theta)\big). \tag{1}$$

Based on Projected Gradient Descent (PGD) adversarial attack [18], PGD AT is arguably a standard means to conduct AT. PGD AT first performs multi-step PGD attacks to approximately solve the inner maximization problem in Eq. (1), where the perturbation crafted by PGD at i-th iteration can be described as

$$\delta^i = \mathcal{P}_\epsilon\Big(\delta^{i-1} + \alpha \cdot \text{sign}\left(\nabla_x f(x+\delta^{i-1};\theta)\right)\Big). \tag{2}$$

The produced adversarial examples are utilized as training data, and the model parameter θ is then updated to minimizing the training loss.

Although PGD AT can withstand strong adversarial attacks, their computational cost is linear to the number of additional adversarial iterations [31], which is extremely computationally expensive in practice. Therefore improving its efficiency has become an active research topic [3], while reducing the number of iterations would be the most straightforward strategy to accelerate the training procedure. In Dynamic Adversarial Training (DAT) [29], the number of adversarial iterations is gradually increased according to a first-order stationary

Table 1: A high-level comparison with previous effect adversarial training methods

Methods	Acceleration strategy	Model independent	Adaptive training	Work with FAST training	Examined on ImageNet
FREE [24]	Update model parameters and adversarial perturbation simultaneously	✓	×	✓	✓
YOPO [35]	Only attack the first layer of trained model to produce training adversarial examples	×	×	×	×
Amata [33]	Linearly increasing the number of adversarial iterations	✓	×	✓	✓
U-FGSM [31]	Single adversarial step with large step size	✓	×	✓	✓
FAT [37]	Conduct early-stop when generating training adversarial examples	✓	✓	×	×
This paper	A self-adaptive dynamic adversarial training framework	✓	✓	✓	✓

condition that measures the training effect. However, DAT needs to initialize the increasing threshold on a pre-trained model with a similar architecture. Based on an annealing mechanism, Amata linearly increases adversarial steps and adjust the adversarial step size during training [33]. As we will show later, determining the optimal training schedules for different training tasks remains difficult. Zhang et al. [35] proposed YOPO, which simplifies the adversarial iteration by only generating adversarial examples toward the first layer of the trained model for adversarial training. Friendly Adversarial Training (FAT) carries out PGD adversaries with an early-stop mechanism to prevent overfitting and reduce training cost [37]. Wong et al. [31] found that one step PGD attack, also known as First Gradient Sign Method (FGSM) [11], with large step size and uniform initialization, could achieve comparable performance to regular PGD AT and be significantly more efficient. They also reported that cyclic learning rate [26] and half-precision computation [19] can significantly boost training efficiency. We refer to training with cyclic learning rate and half-precision computation as FAST training [31], and FGSM AT with uniform initialization as U-FGSM in the rest of this paper. Instead of improving PGD AT, Shafahi et al. [24] proposed a novel training method called FREE, which makes the most use of backpropagation by updating the model parameters and adversarial perturbation simultaneously. This mechanism is called batch replay, and we visualize the process in Fig. 1(a). Table 1 summarizes recent progress in efficient AT and shows the differences between our method and other approaches.

In parallel to efficiency, many efforts have been made to improve AT's effectiveness, *e.g.*, [1, 20, 22]. In this direction, some advanced surrogate loss functions have been proposed to enhance or replace the cross-entropy loss. TRADES can be viewed as a combination of the cross-entropy loss and a KL-divergence based penalty [36]. On top of TRADES, MART merges the cross-entropy loss and the margin loss and pays more attention to misclassified examples [30]. Moreover, Zhang et al. [37] show that these advanced surrogate losses can also benefit from efficient AT methods.

Lipschitz Condition The Lipschitz constant for $f(\cdot;\theta)$ gives an upper bound on how fast the loss value changes when small perturbations are added to the network's input [27]. This concept is closely related to the robustness of DNNs.

Definition 1 (Lipschitz continuity)**.** *Let $\|\cdot\|_a$ and $\|\cdot\|_b$ be two norms on $\mathbb{R}^n$ and $\mathbb{R}$, respectively. We say $f:\mathbb{R}^n \to \mathbb{R}$ is Lipschitz continuous if there exists a Lipschitz constant $K>0$ such that*

$$\|f(x)-f(x+\delta)\|_b \leq K\|\delta\|_a,\ \forall \delta \in B_\epsilon.$$

Assumption 1 (Sinha et al. [25])**.** *Let $\|\cdot\|_p$ be the dual norm of $\|\cdot\|_q$. $f(\cdot;\theta)$ satisfies the Lipschitzian smoothness condition*

$$\left\|\nabla_x f\left(x;\theta\right)-\nabla_x f\left(x+\delta;\theta\right)\right\|_p \leqslant l_{xx}\left\|\delta\right\|_q,\ \forall \delta \in B_\epsilon, \tag{3}$$

where l_{xx} is a positive constant.

Assumption 2 (Deng et al. [9])**.** *Given $f(\cdot;\theta)$ and an example x, there exists a stationary point $x+\delta^* \in B_\epsilon$ such that $\nabla_x f(x+\delta^*;\theta)=0$.*

Given by Definition 1, in this paper, we suppose that the network F and loss function L are Lipschitz continuous [4, 23]. The Lipschitz condition Eq. (3) proposed by Sinha et al.

[25] is commonly used by recent studies [29, 33]. Meanwhile, Deng et al. [9] proved that the gradient-based adversary can find a local maximum that supports the existence of δ^*.

3 Gradient Magnitude Guided Adversarial Training

Previous studies implicitly show that AT is a dynamic procedure [5, 29], which means the number of adversarial iterations to generate suitable perturbation is floating. Thus, we wish to push the efficiency of AT by conducting as few adversarial iterations as possible.

3.1 Motivation and Naive Implementation

To provide an intuitive understanding of the dynamics of AT, we illustrate the learning process in which learned models become more robust. We analyze PGD, U-FGSM, and FREE, three common AT strategies. PGD AT, represented by PGD-AT-7, specifically consists of seven adversarial iterations. FREE is denoted by the notations FREE-4 or FREE-8, indicating that it is performed with four or eight batch replays, respectively. As shown in the first column of Fig. 2, the evaluation performance of PGD-AT-7 and U-FGSM increases linearly throughout the training procedure, indicating that the robustness of models trained by these two approaches is expected to increase monotonically, given that they are only trained on examples perturbed by a fixed adversarial attack method. During FREE AT, on the other hand, the network is trained on clean examples in the first batch replay, and the actual adversarial training starts at the second iteration. However, if the model is adversarially trained repeatedly too many times on a mini-batch, catastrophic forgetting would occur and influence training efficiency [24]. As depicted in the second column of Fig. 2, where the robustness of the FREE-8-trained model swings dramatically throughout adversarial training, the number of iterations required to generate an adequate perturbation appears to fluctuate, and redundant adversarial iteration may also damage the trained models' robustness.

Naive implementation Motivated by the previous observation, we then introduce the Dynamic Efficient Adversarial Training (DEAT) framework, where we wish to push the training efficiency by removing redundant adversarial iteration. Similar to FREE, DEAT starts the training on natural examples via setting the number of batch replay $r = 1$ and gradually increases the number of batch replays to conduct adversarial training in the following training epochs.

DEAT requires a pre-defined criterion to determine the timing of increasing batch replay, which can be achieved in different ways (Pseudocode is presented in Appendix A). Intuitively, performing one extra batch replay every d epoch is a practical and straightforward approach to achieving dynamic adversarial training. We implement DEAT to increase the number of batch replays every 3 epochs, marked by DEAT-3, and present the training process in the third column of Fig. 2. Despite the absence of adversarial robustness in the initial few epochs, the robustness performance of the DEAT-3 trained model shoots up after just one epoch of training on adversarial training examples. In addition to increasing batch replay every few epochs, we notice that training accuracy can also be used to decide when to adjust the number of adversarial iterations. One can observe that as FREE-8's robustness performance diminishes over epoch 2 to epoch 7, its training accuracy rises to 60%, which is remarkably high compared to other techniques, including DEAT-3, whose training accuracy is only slightly above 43%. On the other hand, while the FREE-8-trained model gains robustness during epochs 7 to 10, its training accuracy declines substantially to about 47%. Inspired by this phenomenon, we design another naive implementation of DEAT based on the training accuracy, *i.e.*, adding one more batch replay when the model's training accuracy exceeds the pre-defined threshold. We set the threshold at 40% and execute DEAT accordingly, signified by DEAT-40%. As shown in third column of Fig. 2, DEAT-40% achieves a considerable performance with a smoother learning procedure compared to DEAT-3.

Alongside the robustness performance, it is natural to question DEAT's efficacy. Because the total number of backpropagation, the most computationally expensive operation in AT, can be viewed as a quantification of the training cost [31], we summarize the number of

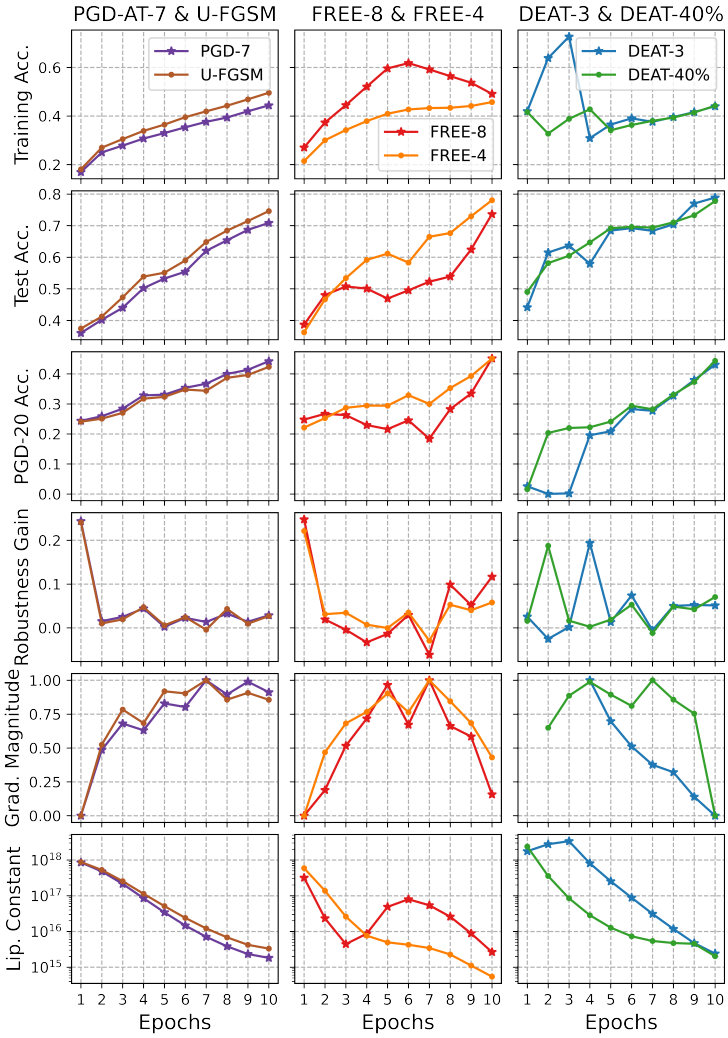

Figure 2: An illustration of the evaluation performance, robustness gain, gradient magnitude, and the Lipschitz constant of models trained by six AT methods. The first three rows show the training accuracy, test accuracy on clean examples, and robustness at each training epoch, where the robustness is tested by the PGD attack with 20 iterations, denoted by PGD-20. The fourth row illustrates the changes in the trained models' robustness relative to the previous epoch. When the robustness gain in one epoch is larger than zero, the trained model is more robust than it was in the previous epoch. The gradient magnitude is shown in the fifth row. The values are normalized for presentation, and a smaller gradient magnitude seems to indicate a more effective training epoch. Because DEAT-3 and DEAT-40% do not perform adversarial training in the first few epochs, we omit the gradient magnitude when the models are only trained on natural examples. The final row displays the upper bound of the Lipschitz constant, which is calculated via the product of each layer's Frobenius norm [4].

Table 2: The number of backpropagation conducted by adversarial training methods in ten epochs, where M is the number of data batches in the training dataset.

Methods	U-FGSM	PGD-AT-7	FREE-4	FREE-8	DEAT-3	DEAT-40%
#Backpropagation	$20M$	$80M$	$40M$	$80M$	$22M$	$25M$

backpropagation of AT methods presented so far in Table 2. Letting M be the number of data batches, U-FGSM and PGD-AT-7 conducted $20M$ and $80M$ times backpropagation in ten training epochs. FREE-8 spent the same amount of computational cost as PGD-AT-7, while

FREE-4 is half cheaper ($40M$) in the same period. By contrast, DEAT-3 only conducted $22M$ times backpropagation, given by $\lceil T(T+d)/2d \rceil$, where T is the total number of epochs, and DEAT-40% performed $25M$ times. Such a performance indicates that DEAT has a significant advantage in training efficiency.

Nevertheless, although both naive implementations perform well in the preliminary test, they are not sufficiently generalizable to various datasets and model architectures. For instance, when doing DEAT-40% on a different training dataset, the training accuracy may never exceed the predefined threshold. If DEAT-3 is conducted with 50 epochs, the last training epoch will have 17 batch replays, which is unacceptable. In order to effectively configure DEAT with these naive criteria for varied training tasks, extensive parameter tuning may be required, hence limiting DEAT's usefulness. To further improve DEAT's generalizability, we need an adaptive strategy that does not rely on manual setup.

3.2 Gradient Magnitude Guided Approach

Recent studies [17, 24, 28] show that the adversarial robustness property is closely related to the geometry of the loss landscape, where AT enhance the trained models' robustness via flatting its loss landscape. In this sense, we propose to utilize the loss curvature of the model as an indicator of the training effect.

Theorem 1. *Given a perturbed example $x+\delta$, where $x \in \mathbb{R}^n$ and $\delta \in B_\epsilon$, if Assumptions 1 and 2 hold, the Lipschitz constant l_{xx} of the first-order derivative of $f(x+\delta;\theta)$ towards training example x satisfies*

$$\frac{\|\nabla_x f\left(x+\delta;\theta\right)\|_1}{2n\epsilon} \leqslant l_{xx}. \tag{4}$$

Recall that l_{xx} in in Eq. (3), a Lipschitz constant of the first-order derivative, implies the curvature around a particular example on the loss landscape by definition. Given by Theorem 1, we show that Eq. (4) gives a reasonable approximation of the Lipschitz constant l_{xx} of $\nabla_x f(x+\delta;\theta)$ within a small ℓ_∞ norm ball [13] (proof is presented in Appendix B). In practice, once the training set X and adversarial threat model are fixed, n and ϵ in Eq. (4) are constants. The flatness around one example can then be measured by $\|\nabla_x f(x+\delta;\theta)\|_1$, and we take an accumulation of the flatness of examples in X, *i.e.*,

$$l_X = \sum_{x \in X} \|\nabla_x f(x+\delta;\theta)\|_1, \tag{5}$$

to quantify the overall curvature of a model.

To see whether gradient magnitude can reflect the training effect, we visualize the gradient magnitude in the fifth row of Fig. 2. For comparison, robustness gain, the changes in the trained models' robustness relative to the previous epoch, and a lose Lipschitz constant of $f(\cdot;\theta)$ at the end of each training epoch are also visualized in the fourth and sixth rows of Fig. 2. Through an epoch-by-epoch comparison in Fig. 2, we can see that the gradient magnitude reflects the effectiveness of each adversarial training epoch precisely. When the robustness of the models increases, the value of gradient magnitude is moderate, but when the robustness decreases, the gradient magnitude of that epoch increases dramatically. In contrast, although a more robust model tends to have a smaller first-order Lipschitz constant [27], the latter can only indicate roughly that an adversarially trained model is becoming more robust but is unable to identify which training epoch was more effective.

While both theoretical and empirical analysis suggests that the trained model gains robustness effectively when gradient magnitude l_X maintains small, how to quantify a threshold for l_X to enable self-adaptive AT remains a question. DAT [29] initializes its threshold via conducting a weak adversarial attack on pre-trained models, while the success of U-FGSM [31] demonstrates that one step attack with uniform initialization could generate qualified training perturbation. Inspired by these previous works, we initialize the increasing threshold to l_X at the second epoch that only contains one adversarial iteration. As described in Algorithm 1, we slightly enlarge the threshold via a relax parameter $\gamma > 1$ at initialization and each update. By doing so, the number of adversarial iteration k will only be increased when the current l_X is strictly larger than in previous epochs. Because $\nabla_x f\left(x+\delta;\theta\right)$ has already been

Algorithm 1 M+: gradient magnitude guided adversarial training.

Require: Training set X, total epochs T, adversarial radius ϵ, step size α, the number of mini-batches M, the number of adversarial iteration k, the evaluation of current training effect l_X and a relax parameter γ

1: $k \leftarrow 0$
2: **for** $t = 1$ to T **do**
3: $\quad l_X \leftarrow 0$
4: $\quad$ **for** $i = 1$ to M **do**
5: $\quad\quad$ Craft adversarial perturbation δ_i via k backpropagation.
6: $\quad\quad$ Save the gradient $\|\nabla_x f(x_i + \delta_i; \theta)\|_1$ at the least iteration.
7: $\quad\quad l_X \leftarrow l_X + \|\nabla_x f(x_i + \delta_i; \theta)\|_1$
8: $\quad\quad$ Update model parameter θ.
9: $\quad$ **end for**
10: $\quad$ **if** $t = 1$ **then**
11: $\quad\quad k \leftarrow k + 1$
12: $\quad$ **else if** $t = 2$ **then**
13: $\quad\quad$ Threshold $\leftarrow \gamma \cdot l_X$
14: $\quad$ **else if** $l_X >$ Threshold **then**
15: $\quad\quad$ Threshold $\leftarrow \gamma \cdot l_X$; $k \leftarrow k + 1$
16: $\quad$ **end if**
17: **end for**

computed in generating adversarial training example, such a criterion only takes a trivial cost to enable the fully automatic training procedure. Furthermore, through the different implementations of the training procedure in lines 5 to 7 of Algorithm 1, we enable the M+ criterion to collaborate with various existing AT methods.

4 Experiments

In this section, we evaluate the proposed methods on the CIFAR-10 and ImageNet datasets. All experiments are built with Pytorch [21] on a workstation that has an Intel i9-9820X processor and 128GB memory. For CIFAR-10 experiments, we use a GeForce RTX 2080Ti, while the ImageNet experiments run on 3 RTX 2080Ti graphics cards.

4.1 A benchmark under a fair training setup

To compare with recently efficient AT methods, we first present a benchmark on the CIFAR-10 dataset under a standard training setup, where all environmental variables are under control except AT methods themselves to make a fair comparison. In addition, TRADES [36], and MART [30] are adopted as advanced surrogate loss functions that can be accelerated [37].

We examine all baselines on PreAct-ResNet 18 [12] and DenseNet 121 [14]. The number of adversarial iterations performed for perturbing training examples has a critical impact on the performance of most baseline methods, therefore, we adopt only the optimal configuration from their original implementations. All methods are carried out 50 epochs with the stochastic gradient descent optimizer and a multi-step learning rate schedule. The detailed setup of training variables and baselines is summarized in Appendix C.1. As for robustness evaluation, we use PGD-i to represent a ℓ_∞ norm-based PGD adversary with i iterations, while CW-i adversary optimizes the margin loss [6] via i PGD steps. The adversarial step size is $2/255$, and the adversarial radio ϵ is $8/255$. The standard AutoAttack [7], denoted by AA, is also included in our evaluation. Each adversarially trained model is tested by a CW-20 adversary on a validation set during training, and we save the most robust checkpoints for the final evaluation [31].

The benchmark is summarized in Table 3. The loss and robustness of trained models are illustrated in Appendix C.4. How M+ methods adjust the number of adversarial iterations is visualized in Appendix D. On the PreAct-ResNet 18, which is one of the most commonly used model architectures in adversarial training literature, we can see that TRADES achieves

Table 3: Evaluation on CIFAR-10 under the standard training setup. We write 'F+' to represent an AT method accelerated by FAT and 'M+' to represent methods accelerated by M+ criterion.

Model Architecture	Method	Natureal	Adversarial			Time
			PGD-100	CW-20	AA	(min)
PreAct ResNet 18	FREE-4	**85.10%**	47.17%	47.11%	43.98	**83.1**
	FREE-6	82.30%	48.27%	47.12%	44.78	124.0
	FREE-8	80.77%	48.54%	47.11%	44.79	162.4
	M+DEAT	83.93%	**48.87%**	**48.12%**	**45.56**	102.1
	PGD-AT-7	82.33%	49.48%	**48.64%**	45.95	157.2
	FAT-5	81.77%	48.65%	47.97%	44.87	92.2
	YOPO-5-3	82.09%	43.02%	43.23%	40.69	**77.8**
	Amata-2-10	79.63%	**50.28%**	48.24%	**46.20**	135.4
	M+PGD	**83.43%**	45.94%	45.66%	42.57	94.8
	TRADES	79.29%	51.06%	48.46%	**47.64**	456.4
	F+TRADES^2	**81.91%**	51.12%	**48.72%**	47.54	**236.0**
	M+TRADES	79.89%	**51.43%**	48.61%	47.52	317.7
	MART	78.04%	54.88%	48.42%	46.67	148.7
	F+MART^2	**84.05%**	49.46%	47.02%	45.46	240.5
	M+MART	78.04%	**55.83%**	**49.19%**	**47.20**	**87.6**
DenseNet 121	FREE-4	**82.81%**	44.83%	44.41%	41.06	**122.4**
	FREE-6	80.68%	46.71%	45.90%	**43.49**	184.5
	FREE-8	79.04%	**46.67%**	**45.76%**	43.22	244.4
	M+DEAT	82.18%	45.16%	45.22%	42.53	152.6
	PGD-AT-7	71.19%	43.40%	41.50%	39.54	220.9
	FAT-5	**75.43%**	41.90%	39.61%	38.57	**168.5**
	YOPO-5-3	-	-	-	-	-
	Amata-2-10	72.10%	43.43%	41.90%	39.77	177.6
	M+PGD	73.06%	**44.28%**	**43.16%**	**40.99**	192.3
	TRADES	70.47%	42.50%	39.30%	38.67	689.1
	F+TRADES^2	**74.33%**	42.75%	39.65%	39.05	499.1
	M+TRADES	72.32%	**43.34%**	**39.77%**	**39.15**	**451.8**
	MART	63.19%	44.62%	39.61%	38.05	330.9
	F+MART^2	**77.39%**	43.35%	40.09%	39.01	434.6
	M+MART	68.33%	**47.46%**	**42.08%**	**40.26**	**132.7**

the best performance on AA test, but it is also the most time-consuming. M+TRADES is 26% faster than TRADES with a similar overall performance, while F+TRADES obtains comparable robustness in half of TRADES's training time. According to Fig. 4(a) and Fig. 6(a), M+TRADES's training efficiency is comparable to F+TRADES's at the early and middle stages, but the increasing adversarial steps slow it down at the final training stage. MART achieves the highest robust performance on the PGD-100 test and is notably faster than TRADES, but there is no substantial improvement on the CW-20 and AA tests. Our M+MART is 40% faster and achieves better robust performance, whereas F+MART is even slower and less robust than the original MART. In the PGD-based group, PGD-AT-7 is a strong baseline under the standard training setup [22] and it outperforms most accelerated AT methods on robustness tests except Amata. As shown in Fig. 6(a), M+PGD only conducts at most 4 backpropagations to generate training adversarial examples, which limits its final robustness performance. M+DEAT is about 35% faster than PGD-AT-7 and achieves comparable robustness regarding the CW-20 and AA tests. FREE-6 is more efficient than FREE-8 and shows similar robustness, M+DEAT is about 17% faster than FREE-6 and has higher accuracy on all evaluation tasks. As demonstrated by Fig. 4(a) and Fig. 6(a), M+DEAT performs fewer batch replays than other FREE methods at the early training stage, resulting in a large reduction in time consumption, which is to be expected.

Because DenseNet 121 have received less attention in the literature on adversarial training, existing AT approaches that rely on manual setup cannot perform adequately on this

model. Our M+ acceleration, on the other hand, overcomes the limitations imposed by manual adjustment and enables its cooperative methods to attain better performance in this benchmark. AT methods combined with our M+ acceleration achieve significantly better results than their original implementation regarding computing cost and AA score. How M+ methods change the number of adversarial iterations on DenserNet 121 is displayed in Fig. 6(b). Due to the space limitation, the evaluation under FAST training setup is presented in Appendix C.2, while the empirical analysis of hyper-parameters and an ablation studies of training tricks are presented in Appendix C.3.

4.2 Evaluation on ImageNet

In this section, we evaluate the M+DEAT on the ImageNet. Because the classical AT method could take thousands of GPU hours to adversarially train an ImageNet classifier [32], we consider FREE-4 as the baseline method, which finishes training within a reasonable amount of time and achieves the better robustness than PGD AT [24]. Although U-FGSM can also work on ImageNet, its training procedure includes several tricks, *i.e.*, three training phases with different levels of cropping and learning rate schedules. Due to too many manual factors, U-FGSM is not considered as a baseline here. Because Ye et al. [33] did not release the implementation of the Amata method. We only list their result on ImageNet for accuracy comparison. To make a fair comparison, we use the same training setting as FREE-4's original implementation, *i.e.*, SGD optimizer and a multi-step learning rate schedule, where the momentum and weight decay are 0.9 and 10^{-4} respectively, and the learning rate starts at 0.1 and is decayed at 9 and 17 epochs by a factor of 10.

As shown in Table 4, M+DEAT can work properly on ImageNet and the acceleration effect is considerable. Compared to FREE-4, M+DEAT is about 34% faster and shows similar levels of robustness when $\gamma = 1.1$. Because a small γ could introduce more adversarial iterations, M+DEAT with $\gamma = 1.01$ is only 16% faster than FREE-4, but it achieves slightly better performance on robustness tests.

Table 4: Results of ResNet 50 on ImageNet ($\epsilon = 4/255$).

Method	Natural	PGD-10	PGD-50	Time (h.)
FREE-4	61.02%	31.90%	30.93%	52.43
Amata-2-4 [33]	59.7%	31.8%	31.2%	-
M+DEAT				
$\gamma = 1.1$	62.04%	31.40%	30.18%	34.34
$\gamma = 1.01$	60.10%	32.34%	31.41%	44.67

5 Conclusion and Future Work

In this paper, we demonstrate that the gradient magnitude can indicate the effect of adversarial training and design a self-adaptive acceleration strategy, called M+ acceleration, accordingly. M+ acceleration can easily collaborate with state-of-the-art adversarial training approaches to improve their training efficiency. Comprehensive experiments have been done on CIFAR-10 and ImageNet datasets to evaluate the efficiency and effectiveness of the proposed method, where M+ acceleration performs exceptionally well with various training setups, demonstrating its generalizability and adaptability.

This work has mainly explored ℓ_∞ norm-based adversarial training, so one of the future works is to generalize the magnitude guided strategy into threat models under other metrics. We believe that the ultimate goal of this direction would be an efficient adversarial training framework that can work under multiple threat models on various deep learning tasks. Besides, the potential collaboration between our strategy and other efficient adversarial training methods, *e.g.*, [33, 35] will also be explored in our future works.

References

[1] M. Andriushchenko and N. Flammarion. Understanding and improving fast adversarial training. In *Advances in Neural Information Processing Systems (NeurIPS)*, Virtual Event, December 6-12, 2020.

[2] A. Athalye, N. Carlini, and D. A. Wagner. Obfuscated gradients give a false sense of security: Circumventing defenses to adversarial examples. In *International Conference on Machine Learning (ICML)*, Stockholmsmässan, Stockholm, Sweden, July 10-15, 2018.

[3] T. Bai, J. Luo, J. Zhao, B. Wen, and Q. Wang. Recent advances in adversarial training for adversarial robustness. In *International Joint Conference on Artificial Intelligence (IJCAI)*, Virtual Event / Montreal, Canada, August 19-27, 2021.

[4] P. L. Bartlett, D. J. Foster, and M. Telgarsky. Spectrally-normalized margin bounds for neural networks. In *Advances in Neural Information Processing Systems (NeurIPS)*, Long Beach, CA, USA, December 4-9, 2017.

[5] Q. Cai, C. Liu, and D. Song. Curriculum adversarial training. In *International Joint Conference on Artificial Intelligence (IJCAI)*, Stockholm, Sweden, July 13-19, 2018.

[6] N. Carlini and D. Wagner. Towards evaluating the robustness of neural networks. In *Symposium on Security and Privacy, SP*, San Jose, CA, USA, May 22-26, 2017.

[7] F. Croce and M. Hein. Reliable evaluation of adversarial robustness with an ensemble of diverse parameter-free attacks. In *International Conference on Machine Learning (ICML)*, Virtual Event, July 13-18, 2020.

[8] J. Deng, W. Dong, R. Socher, L.-J. Li, K. Li, and L. Fei-Fei. Imagenet: A large-scale hierarchical image database. In *Conference on Computer Vision and Pattern Recognition (CVPR)*, Miami, Florida, USA, June 20-25, 2009.

[9] Z. Deng, H. He, J. Huang, and W. J. Su. Towards understanding the dynamics of the first-order adversaries. In *International Conference on Machine Learning (ICML)*, Virtual Event, July 13-18, 2020.

[10] Y. Dong, Q. Fu, X. Yang, T. Pang, H. Su, Z. Xiao, and J. Zhu. Benchmarking adversarial robustness on image classification. In *Conference on Computer Vision and Pattern Recognition (CVPR)*, Seattle, WA, USA, June 13-19, 2020.

[11] I. J. Goodfellow, J. Shlens, and C. Szegedy. Explaining and harnessing adversarial examples. In *International Conference on Learning Representations (ICLR)*, San Diego, CA, USA, May 7-9, 2015.

[12] K. He, X. Zhang, S. Ren, and J. Sun. Identity mappings in deep residual networks. In *European Conference on Computer Vision (ECCV)*, Amsterdam, The Netherlands, October 11-14, 2016.

[13] J. Heinonen. *Lectures on Lipschitz analysis*. University of Jyväskylä., 2005.

[14] G. Huang, Z. Liu, L. van der Maaten, and K. Q. Weinberger. Densely connected convolutional networks. In *Conference on Computer Vision and Pattern Recognition (CVPR)*, Honolulu, HI, USA, July 21-26, 2017.

[15] X. Huang, D. Kroening, W. Ruan, J. Sharp, Y. Sun, E. Thamo, M. Wu, and X. Yi. A survey of safety and trustworthiness of deep neural networks: Verification, testing, adversarial attack and defence, and interpretability. *Computer Science Review*, 37:100270, 2020.

[16] A. Krizhevsky. Learning multiple layers of features from tiny images, 2009. URL `https://www.cs.toronto.edu/~kriz/cifar.html`.

[17] X. Liu, M. Cheng, H. Zhang, and C. Hsieh. Towards robust neural networks via random self-ensemble. In *European Conference on Computer Vision (ECCV)*, Munich, Germany, September 8-14, 2018.

[18] A. Madry, A. Makelov, L. Schmidt, D. Tsipras, and A. Vladu. Towards deep learning models resistant to adversarial attacks. In *International Conference on Learning Representations (ICLR)*, Vancouver, BC, Canada, April 30 - May 3, 2018.

[19] P. Micikevicius, S. Narang, J. Alben, et al. Mixed precision training. In *International Conference on Learning Representations, (ICLR)*, Vancouver, BC, Canada, April 30 - May 3, 2018.

[20] T. Pang, X. Yang, Y. Dong, H. Su, and J. Zhu. Bag of tricks for adversarial training. In *International Conference on Learning Representations (ICLR)*, Virtual Event, Austria, May 3-7, 2020.

[21] A. Paszke, S. Gross, F. Massa, et al. Pytorch: An imperative style, high-performance deep learning library. In *Advances in Neural Information Processing Systems (NeurIPS)*, Vancouver, BC, Canada, December 8-14, 2019.

[22] L. Rice, E. Wong, and J. Z. Kolter. Overfitting in adversarially robust deep learning. In *International Conference on Machine Learning (ICML)*, Virtual Event, July 13-18, 2020.

[23] W. Ruan, X. Huang, and M. Kwiatkowska. Reachability analysis of deep neural networks with provable guarantees. In *International Joint Conference on Artificial Intelligence (IJCAI)*, pages 2651–2659, Stockholm, Sweden, July 13-19, 2018.

[24] A. Shafahi, M. Najibi, A. Ghiasi, Z. Xu, J. P. Dickerson, C. Studer, L. S. Davis, G. Taylor, and T. Goldstein. Adversarial training for free! In *Advances in Neural Information Processing Systems (NeurIPS)*, Vancouver, BC, Canada, December 8-14, 2019.

[25] A. Sinha, H. Namkoong, and J. C. Duchi. Certifying some distributional robustness with principled adversarial training. In *International Conference on Learning Representations, (ICLR)*, Vancouver, BC, Canada, April 30 - May 3, 2018.

[26] L. N. Smith and N. Topin. Super-convergence: Very fast training of neural networks using large learning rates, 2018. Preprint at `https://arxiv.org/abs/1708.07120`.

[27] C. Szegedy, W. Zaremba, I. Sutskever, J. Bruna, D. Erhan, I. J. Goodfellow, and R. Fergus. Intriguing properties of neural networks. In *International Conference on Learning Representations (ICLR)*, Banff, AB, Canada, April 14-16, 2014.

[28] J. Wang and H. Zhang. Bilateral adversarial training: Towards fast training of more robust models against adversarial attacks. In *International Conference on Computer Vision (ICCV)*, Seoul, Korea (South), October 27 - November 2, 2019.

[29] Y. Wang, X. Ma, J. Bailey, J. Yi, B. Zhou, and Q. Gu. On the convergence and robustness of adversarial training. In *International Conference on Machine Learning (ICML)*, Long Beach, CA, USA, June 9-15, 2019.

[30] Y. Wang, D. Zou, J. Yi, J. Bailey, X. Ma, and Q. Gu. Improving adversarial robustness requires revisiting misclassified examples. In *International Conference on Learning Representations (ICLR)*, Virtual Event, Austria, May 3-7, 2020.

[31] E. Wong, L. Rice, and J. Z. Kolter. Fast is better than free: Revisiting adversarial training. In *International Conference on Learning Representations (ICLR)*, Addis Ababa, Ethiopia, April 26-30, 2020.

[32] C. Xie, Y. Wu, L. v. d. Maaten, A. L. Yuille, and K. He. Feature denoising for improving adversarial robustness. In *Conference on Computer Vision and Pattern Recognition (CVPR)*, Long Beach, CA, USA, June 16-20, 2019.

[33] N. Ye, Q. Li, X. Zhou, and Z. Zhu. Amata: An annealing mechanism for adversarial training acceleration. In *Conference on Artificial Intelligence (AAAI)*, Virtual Event, February 2-9, 2021.

[34] S. Zagoruyko and N. Komodakis. Wide residual networks. In *British Machine Vision Conference (BMVC)*, York, UK, September 19-22, 2016.

[35] D. Zhang, T. Zhang, Y. Lu, Z. Zhu, and B. Dong. You only propagate once: Accelerating adversarial training via maximal principle. In *Advances in Neural Information Processing Systems (NeurIPS)*, Vancouver, BC, Canada, December 8-14, 2019.

[36] H. Zhang, Y. Yu, J. Jiao, E. P. Xing, L. E. Ghaoui, and M. I. Jordan. Theoretically principled trade-off between robustness and accuracy. In *International Conference on Machine Learning (ICML)*, Long Beach, CA, USA, June 9-15, 2019.

[37] J. Zhang, X. Xu, B. Han, G. Niu, L. Cui, M. Sugiyama, and M. S. Kankanhalli. Attacks which do not kill training make adversarial learning stronger. In *International Conference on Machine Learning (ICML)*, Virtual Event, July 13-18, 2020.

Checklist

1. For all authors...
   (a) Do the main claims made in the abstract and introduction accurately reflect the paper's contributions and scope? [Yes]
   (b) Did you describe the limitations of your work? [Yes]
   (c) Did you discuss any potential negative societal impacts of your work? [N/A]
   (d) Have you read the ethics review guidelines and ensured that your paper conforms to them? [Yes]
2. If you are including theoretical results...
   (a) Did you state the full set of assumptions of all theoretical results? [Yes]
   (b) Did you include complete proofs of all theoretical results? [Yes]
3. If you ran experiments...
   (a) Did you include the code, data, and instructions needed to reproduce the main experimental results (either in the supplemental material or as a URL)? [Yes]
   (b) Did you specify all the training details (e.g., data splits, hyperparameters, how they were chosen)? [Yes]
   (c) Did you report error bars (e.g., with respect to the random seed after running experiments multiple times)? [Yes]
   (d) Did you include the total amount of compute and the type of resources used (e.g., type of GPUs, internal cluster, or cloud provider)? [Yes]
4. If you are using existing assets (e.g., code, data, models) or curating/releasing new assets...
   (a) If your work uses existing assets, did you cite the creators? [Yes]
   (b) Did you mention the license of the assets? [Yes]
   (c) Did you include any new assets either in the supplemental material or as a URL? [No]
   (d) Did you discuss whether and how consent was obtained from people whose data you're using/curating? [N/A]
   (e) Did you discuss whether the data you are using/curating contains personally identifiable information or offensive content? [N/A]
5. If you used crowdsourcing or conducted research with human subjects...
   (a) Did you include the full text of instructions given to participants and screenshots, if applicable? [N/A]
   (b) Did you describe any potential participant risks, with links to Institutional Review Board (IRB) approvals, if applicable? [N/A]
   (c) Did you include the estimated hourly wage paid to participants and the total amount spent on participant compensation? [N/A]

A Pseudocode of DEAT

Algorithm 2 Dynamic Efficient Adversarial Training

Require: Training set X, total epochs T, adversarial radius ϵ, step size α, the number of mini-batches M, and the number of batch replay r

```
Initialize the number of batch replay: r ← 1                ▷ Start training on clean examples
for t = 1 to T do
    for i = 1 to M do
        Initialize perturbation δ_i
        for j = 1 to r do                                   ▷ Adversarial training starts when j = 2
            ∇_x, ∇_θ ← ∇L(F(x_i + δ_i; θ))
            θ ← θ − ∇_θ                                     ▷ Apply gradient descent
            δ ← P_ε(δ + α · sign(∇_x))
        end for
    end for
    if meet increase criterion then
        r ← r + 1                   ▷ Add one more batch replay since the following epoch
    end if
end for
```

B Proof of Theorem 1

Recall that

Theorem 1. *Given a perturbed example $x+\delta$, where $x \in \mathbb{R}^n$ and $\delta \in B_\epsilon$, if Assumptions 1 and 2 hold, the Lipschitz constant l_{xx} of the first-order derivative of $f(x+\delta;\theta)$ towards training example x satisfies*

$$\frac{\|\nabla_x f(x+\delta;\theta)\|_1}{2n\epsilon} \leqslant l_{xx}.$$

Proof. Substituting $x+\delta$ and the stationary point $x+\delta^*$ into Eq. (3) gives

$$\|\nabla_x f(x+\delta;\theta) - \nabla_x f(x+\delta^*;\theta)\|_1 \leqslant l_{xx} \|\delta - \delta^*\|_\infty . \tag{6}$$

Because $x+\delta^*$ is a stationary point and $\nabla_x f(x+\delta^*;\theta) = 0$, the left side of Eq. (6) can be written as $\|\nabla_x f(x+\delta;\theta)\|_1$. The right side of Eq. (6) can be simplified as

$$\begin{aligned} \|\delta - \delta^*\|_\infty &\leqslant l_{xx} (\|\delta\|_\infty + \|\delta^*\|_\infty) \\ &\leqslant l_{xx} \cdot (2\epsilon|x|) . \end{aligned} \tag{7}$$

The first inequality holds because of the triangle inequality, and the last inequality holds because both $\|\delta\|_\infty$ and $\|\delta^*\|_\infty$ are upper bounded by B_ϵ that is given by $\epsilon|x|$. So Eq. (6) can be written as Eq. (4). This concludes the proof. □

C Additional Experiments

C.1 Experiment setup in Section 4.1

This benchmark includes two model architectures, *i.e.*, PreAct-ResNet 18 and DenseNet 121. All models are trained with 50 epochs, where we use the stochastic gradient descent optimizer and a multi-step learning rate schedule, where the learning rate is decayed at 25 and 40 epochs. The initial learning rate for PreAct-ResNet 18 is 0.05, however, DenseNet 121 fail to converge when trained with the same learning rate as PreAct-ResNet 18. Therefore, we set their initial learning rate at 0.01. All training hyper-parameters are reported in Table 5.

In Tab. 3, FAT [37] is carried out with 5 maximum training adversarial iterations. According to [36, 37], both original TRADES and FAT with TRADES surrogate loss, denoted by F+TRADES, use 10 adversarial steps. The same number of adversarial steps is also applied

Table 5: Detailed setup for the standard training benchmark in Sec. 4.1

Setup		Model architectures	
		PreAct ResNet 18	DenseNet 121
Training	Initial learning rate	0.05	0.01
	Total epochs	50	
	Learning rate schdule	Multi-step learning rate, where the learning rate is decayed at 25 and 40 epochs	
	Batch size	128	
Optimization	Optimizer	Stochastic Gradient Descent	
	Momentum	0.9	
	Weight decay	0.0005	

in the original MART and FAT with MART surrogate loss (F+MART), which is the same setup used by [30]. As for the hyper-parameter τ, which controls the early stop procedure in FAT, we conduct the original FAT, F+TRADES and F+MART at $\tau = 3$, which enables their highest robust performance [37]. Furthermore, YOPO-5-3 [35] performs 3 backpropagations to update training adversarial examples and repeats such a procedure 5 times. Amata-2-10 [33] linearly increases the number of adversarial iterations from 2 to 10 during training. FREE is performed with three different numbers of batch replays, where FREE-8 conducts 8 batch replays and would show better robustness, while FREE-4 only does 4 batch replays and should be relatively more efficient [24]. All gradient magnitude accelerated methods, namely M+DEAT, M+PGD, M+TRADES, and M+MART, are performed at $\gamma = 1.01$, which is the relax parameter.

C.2 Utilizing the FAST training setup

To demonstrate M+DEAT's adaptability, we compare it with two naive DEAT methods, FREE-4, FREE-8, and PGD-AT-7 under the FAST Training Setup on CIFAR-10 and report the evaluation results. Recall that the FAST training setup was proposed by [31], which utilizes the cyclic learning rate [26] and half-precision computation [19] to speed up adversarial training. Here, the maximum of the cyclic learning rate is carried out at 0.1. As a reminder, DEAT-3 increases the number of batch replays every three epochs, and DEAT-40% determines the timing of increase based on the training accuracy. All DEAT methods are evaluated at step size $\alpha = 10/255$. We set $\gamma = 1$ for PreAct-ResNet and $\gamma = 1.01$ for Wide-ResNet [34]. All methods are carried out with 10 adversarial training epochs. Because DEAT methods start training on natural examples, DEAT-3 has 12 training epochs in total, and DEAT-40% and M+DEAT run 11 epochs. We report the average performance of these methods on three random seeds.

The results on PreAct-ResNet 18 are shown in Table 6, and we can see that all DEAT methods perform properly under the FAST training setup. Among three DEAT methods, models trained by M+DEAT show the highest robustness. Because of the increasing number of batch replay at the later training epochs, M+DEAT performs more backpropagations to finish training, so it spends slightly more training time. FREE-4 achieves a comparable robust performance to M+DEAT, but M+DEAT is 20% faster and has higher classification accuracy on the natural test set. The time consumption of FREE-8 almost triples those two DEAT methods, but it only achieves a similar amount of robustness to DEAT-3. PGD-AT-7 uses the same number of backpropagations as FREE-8 but performs worse.

The comparison on Wide-ResNet [34] model also provides a similar result. The evaluation results on Wide-ResNet 34 architecture are presented in Table 7. We can see that most methods perform better than before because Wide-ResNet 34 is more complex and has more parameters than PreAct-ResNet 18. Although FREE-8 achieves the highest overall robustness, its training cost is much more expensive than others. Compared to FREE-8, FREE-4 is half cheaper than FREE-8 and also performs considerably. M+DEAT is 22% faster than FREE-4 with comparable robustness and achieves 97% training effect of FREE-8 with 40% time consumption. Other DEAT methods are faster than M+DEAT because fewer

backpropagations have been conducted. Models trained by them show reasonable robustness on all tests, but their performance is not as good as that of M+DEAT. Please note that the experiment on Wide-ResNet is meant to demonstrate the generalizability of M+ acceleration, not to challenge the robustness record.

Table 6: Evaluation on CIFAR-10 with PreAct-ResNet 18 under FAST training setup.

Method	Natural	Adversarial				Time
		FGSM	PGD-100	CW-20	AA	(min)
DEAT-3	**80.09%**	49.75%	42.94%	42.26%	40.17	5.8
DEAT-40%	79.52%	48.64%	42.81%	42.08%	40.06	**5.6**
M+DEAT	79.88%	**49.84%**	43.38%	**43.36%**	**41.18**	6.0
FREE-4	78.46%	49.52%	43.97%	43.16%	40.65	7.8
FREE-8	74.56%	48.60%	**44.11%**	42.49%	40.72	15.7
PGD-AT-7	70.90%	46.37%	43.17%	41.01%	40.29	15.1

Table 7: Evaluation on CIFAR-10 with Wide-ResNet 34 under FAST training setup.

Method	Natural	Adversarial				Time
		FGSM	PGD-100	CW-20	AA	(min)
DEAT-3	81.58%	50.53%	44.39%	44.43%	43.50	41.6
DEAT-40%	81.49%	51.08%	45.03%	44.49%	42.50	**38.9**
M+DEAT	**81.59%**	51.29%	45.27%	45.09%	44.45	43.1
FREE-4	80.34%	**51.72%**	46.17%	45.62%	43.30	55.4
FREE-8	77.69%	51.45%	**46.99%**	**46.11%**	**44.90**	110.8
PGD-AT-7	72.12%	47.39%	44.80%	42.18%	41.95	109.1

Comparing to U-FGSM Here, we report the competition between DEAT and U-FGSM. The comparison is summarized in Table 8. We can see that the differences in robustness performance between U-FGSM and DEAT methods are subtle under the FAST training setup. They achieve a similar balance between robustness and time consumption, while M+DEAT performs better on most tests but also takes slightly more training time. When using the standard training setup, U-FGSM is faster but only achieves a fair robust performance.

C.3 Empirical analysis

In this section, we explore the impact of two hyper-parameters, *i.e.*, step size α and relax parameter γ, and conduct ablation studies on several tricks involved in the benchmark under the standard training setup.

The impact of hyper-parameters α and γ Under the FAST training setup, we evaluate the trained models' performance with different step sizes at $\gamma \in \{1.1, 1.01, 1.001\}$. Each model is trained with 10 epochs, and each combination of α and γ has been tested on 5 random seeds. To highlight the relationship between models' robustness and the corresponding training cost, which is denoted by the number of backpropagations (#BP), we use PGD-20 error that is computed as one minus the model's classification accuracy on PGD-20 adversarial examples. The result has been summarized in Fig. 3. This experiment shows that the models' robustness is more sensitive to α rather than γ. We can also see that M+DEAT achieves a slightly better robustness performance when using a large step size, e.g., 14/255, but the corresponding training cost is much higher than that with a lower step size when γ is small.

Ablation studies of three training tricks The default training tricks in Table 3 are multi-step learning rate, uniformly initialized perturbation, and slightly enlarge the step size α. Under the standard training setup, we investigate whether these tricks are truly effective for M+DEAT. In addition to simply removing these tactics, we also evaluate an

Table 8: Compare M+DEAT to U-FGSM under different setups on CIFAR-10.

Set up	Method	Natural	PGD-100	CW-20	AA	Time (min)
PreAct-Res.	M+DEAT	79.88%	43.38%	43.36%	41.18	6.0
+ FAST	U-FGSM	78.45%	43.86%	43.04%	39.80	5.6
Wide-Res.	M+DEAT	81.59%	45.27%	45.09%	44.45	43.1
+ FAST	U-FGSM	80.89%	45.45%	44.91%	42.45	41.3
PreAct-Res.	M+DEAT	83.93%	48.87%	48.12%	45.56	102.1
+ Standard	U-FGSM	81.99%	45.77%	45.74%	42.25	40.3

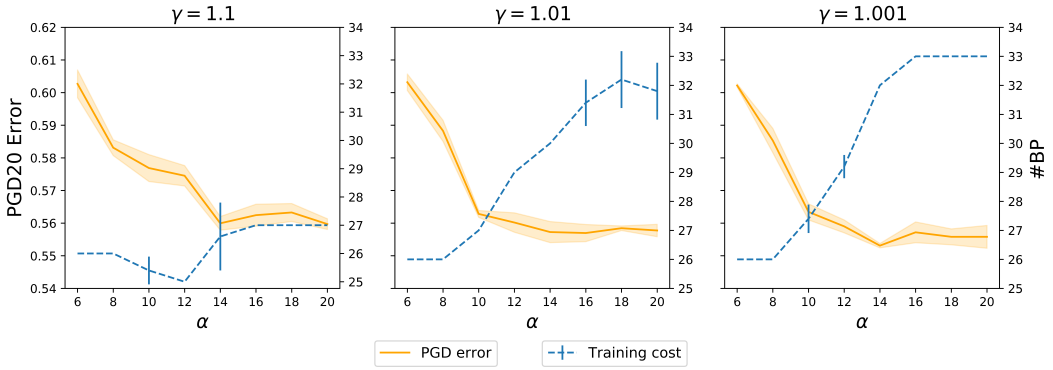

Figure 3: Visualize the impact of α and γ. #BP is a shorthand for the number of backpropagations. PGD-20 error is computed as one minus model's classification accuracy of PGD-20 adversarial examples.

alternative for each. For the learning rate schedule, we consider the flat learning rate and cyclic learning rate. The perturbation initialization is performed with zero initialization and normally random initialization. The step size α is additionally carried out at 8/255 and 12/255. It can be seen from Table 9 that the flat learning rate significantly weakens performance across the board, indicating that a dynamic learning rate schedule is necessary to accelerate training convergence. Comparing cyclic learning rate with multi-step learning rate, M+DEAT with the former achieves marginally better robustness performance with 10% longer runtime. In terms of robustness performance, uniform initialization surpasses normal and zero initialization, whereas zero initialization is actually better than normal initialization. The most appropriate step size is 10/255. In the meantime, enlarging the step size raises the computational cost of M+DEAT. Such an effect can also be observed in Fig. 3.

Table 9: Ablation studies of learning rate schedule, perturbation initialization, and step size with M+DEAT trained PreAct ResNet 18 on CIFAR-10.

Learning rate schedule			Perturbation init.			Step size α (·/255)			Natural	PGD-100	CW-20	Time
Multi-step	Cyclic	Flat	Uniform	Normal	Zero	8	10	12				
✓			✓			✓			83.72%	47.97%	47.66%	92.8
✓			✓					✓	83.67%	48.59%	47.98%	108.9
✓					✓		✓		81.95%	49.27%	47.65%	105.1
✓				✓			✓		**85.73%**	45.87%	46.37%	**81.6**
	✓		✓				✓		83.97%	**49.24%**	**48.65%**	116.4
		✓	✓				✓		66.20%	35.41%	34.95%	100.3
✓			✓				✓		83.93%	48.87%	48.12%	102.1

C.4 Visualization of training process in Sec 4.1

The adversarial training on PreAct-ResNet 18 is illustrated in Fig. 4 in terms of validation accuracy and training loss.

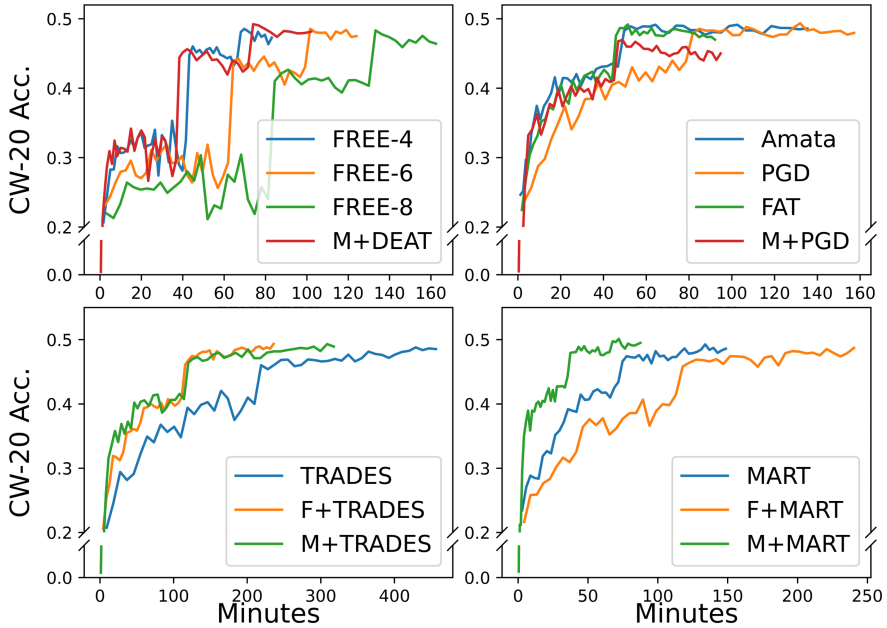

(a) Validation Accuracy

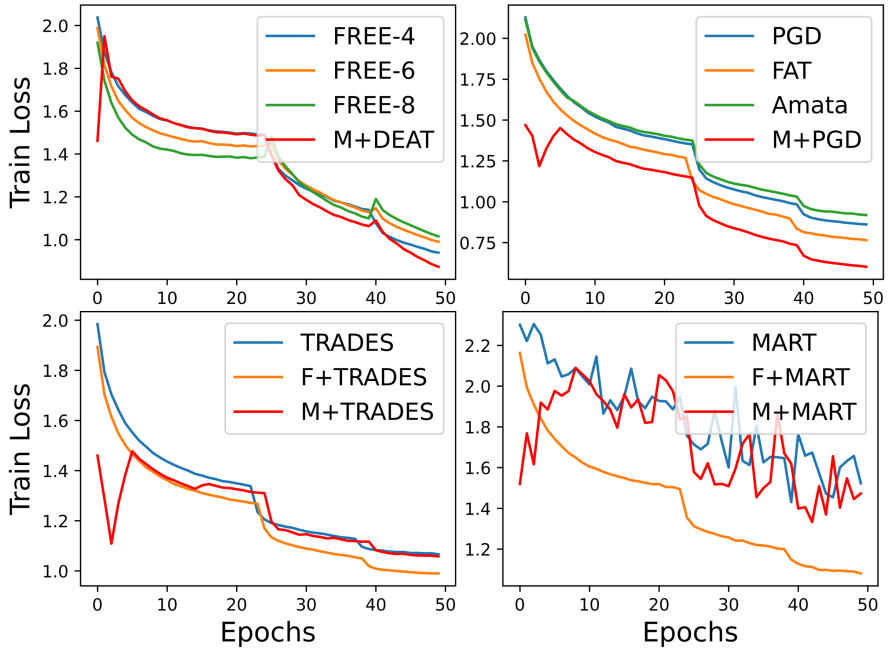

(b) Training Loss

Figure 4: An illustration about how adversarially trained PreAct-ResNet 18 gain robustness (a) and how their training loss changes (b).

The adversarial training on DenseNet 121 is illustrated in Fig. 4 in terms of validation accuracy and training loss.

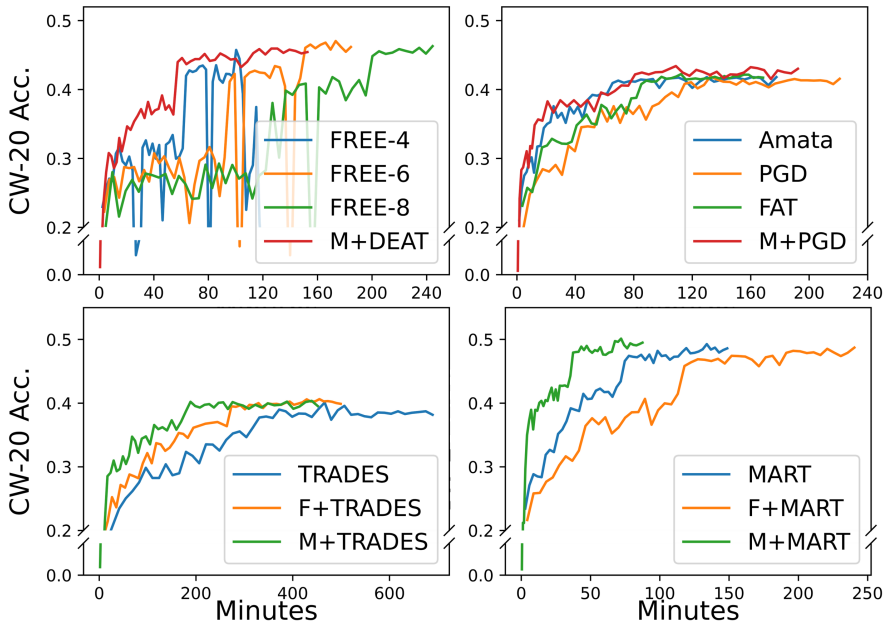

(a) Validation Accuracy

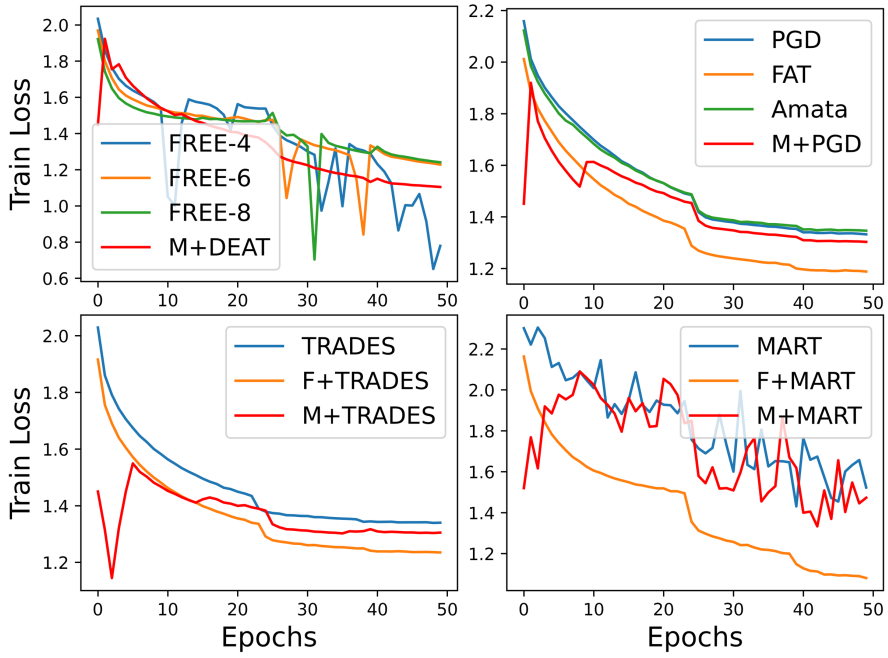

(b) Training Loss

Figure 5: An illustration about how adversarially trained DenseNet 121 gain robustness (a) and how their training loss changes (b).

D Visualization of how the number of backpropagations change in M+ methods

M+ acceleration allows its cooperative methods to increase the number of adversarial iterations during training, resulting in less backpropagation and increased efficiency. To illustrate the adversarial training process of M+ techniques, we display in Fig. 6 the number of backpropagation operations performed by these methods.

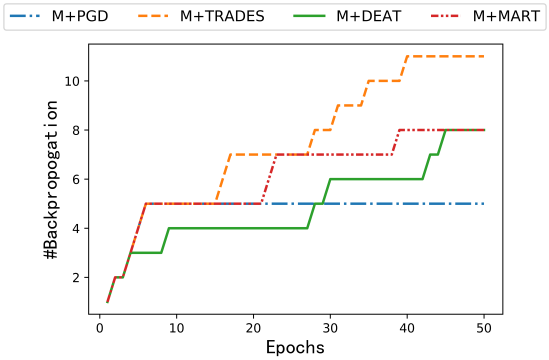

(a) PreAct-ResNet 18

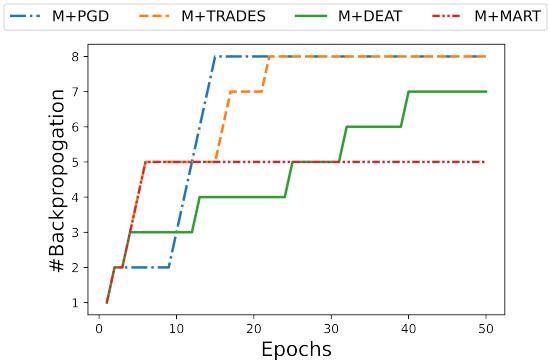

(b) DenseNet 121

Figure 6: The number of backpropagations with respect to epochs.